Structure and function of the UVDE repair protein

Paspaleva, K.

Active site organisation of UVDE - a Mn^{2+} dependent nuclease

Chapter 5

Keti Paspaleva, Geri F. Moolenaar, Nora Goosen

Laboratory of molecular genetics, Leiden Institute of Chemistry, Gorlaeus Laboratories, Leiden University, Einsteinweg 55, 2300 RA Leiden, The Netherlands

SUMMARY

UV damage endonuclease (UVDE) initiates an alternative repair pathway for UV lesions by introducing a nick immediately 5' to both cyclobutane pyrimidine dimers and 6-4 photoproducts. Discovered for the first time in *Schizosaccharomyces pombe*, a broad substrate specificity has been proposed for this nuclease, including not only UV lesions, but also abasic sites, single strand nicks and thymine glycols. By comparing the activity of UVDE proteins from *Schizosaccharomyces pombe* (Spo), *Bacillus subtilis* (Bsu) and *Thermus thermophilus* (Tth) we show that the broad substrate specificity is restrained to the eukaryotic Spo homologue, while the Tth-UVDE functions as an UV damage specific repair enzyme. In this paper we give clear evidence that Mn^{2+} is the catalytic cofactor for all three UVDE proteins. We propose that full occupation of the UVDE metal binding site occurs only after DNA binding. We show that for the Spo- and the Bsu-UVDE Mg^{2+} has a specific role in reducing the non-specific DNA binding. In contrast, for the Tth enzyme Mg^{2+} is shown to inhibit the protein activity by competing with Mn^{2+} in the active site. We further show that the inability of Bsu-UVDE to incise DNA containing a thymine glycol or a single strand nick is not due to lack of damage recognition. Instead, after binding to these lesions the Bsu protein fails to induce the required destacking of the bases opposite the damage.

INTRODUCTION

Ultraviolet light induces two major types of DNA damage: cyclobutane pyrimidine dimers (CPDs) and (6-4) photoproducts (6-4PP). To ensure cell survival, various DNA repair pathways have evolved to remove these lesions. One effective mechanism is the UV damage endonuclease (UVDE), where a single UVDE enzyme recognises and subsequently nicks DNA containing a CPD or a 6-4PP. UVDE was identified for the first time in the fission yeast *Schizosaccharomyces pombe* (Bowman *et al*., 1994). Initially broad substrate specificity has been suggested for this nuclease, including not only UV lesions, but also abasic sites and some nucleotide mismatches (Kanno *et al*., 1999), (Kaur *et al*., 1999). Later studies, however, revealed that the *S. pombe* UVDE recognises the abasic site in a sequence dependent manner, with a very low activity when the damage is flanked by two purines (Paspaleva *et al*., 2009).

UVDE orthologues have been discovered in a number of fungi and eubacterial species, as well as in four archaebacteria (Goosen and Moolenaar, 2008). On the amino acid level there are some intriguing differences between the pro- and eukaryotic proteins, since the bacterial UVDEs are notably shorter and lack the N-terminal 200 amino acids. The C-terminal part of the protein is also not conserved and varies in length (Goosen and Moolenaar, 2008).

The structure of *T. thermophilus* UVDE, solved with 1.55 Å resolution, revealed significant similarities with the BER enzyme Endonuclease IV, both being TIM-barrel metal dependent nucleases (Paspaleva *et al*., 2007). It is currently believed that the catalytic mechanism of UVDE might be very similar to the one of Endo IV, where the DNA is cleaved with the help of trimetal Zn^{2+} cluster (Hossfield *et al*., 1999).

In the UVDE structure the catalytic site was also seen to have the potential to accommodate three ions, although due to low occupation, the anomalous density maps failed to elucidate their nature. Crystallisation in the presence of Mn^{2+} ions yielded structure with improved occupancies of the active site metals, highly suggesting that Mn^{2+} is able to bind within the enzyme catalytic site (Meulenbroek *et al.*, 2009). Biochemical tests further supported this hypothesis, since Mn^{2+} was seen to be requirement for the *T. thermophilus* UVDE catalytic activity (Paspaleva *et al.*, 2007). The UVDE active site metals superimpose on the three zinc sites of Endo IV (Paspaleva *et al.,* 2007), implying that Mn1 and/or Mn2 may be involved in creating the water derived nucleophile.

Interestingly, although the crystal structure of Endo IV reveals the presence of three Zn^{2+} ions, previous data suggest that for its function it can use other divalent metals such as Mn^{2+} (Levin *et al.*, 1988), Co^{2+} (Levin *et al.*, 1991) and Mg^{2+} (Kutyavin *et al.*, 2006). Although Mn^{2+} was proposed as a possible cofactor for the *T. thermophilus* UVDE, little is known about the ionic requirements of UVDE in other organisms. The vast majority of biochemical tests with the *S. pombe* homologue have been performed with a combination of 1 mM Mn^{2+} and 10 mM Mg^{2+} in the reaction mix (reviewed in Doetch *et al*., 2006). In some studies (Kanno *et al*., 1999) only Mg^{2+} was utilized, showing that the *S. pombe* protein can use this metal ion as a catalytic

cofactor. For the *T. thermophilus* UVDE, however, Mg^{2+} is not able to stimulate the enzymatic activity (Paspaleva *et al*., 2007) and the UVDE from *Deinococcus radiodurans* was also reported to specifically require Mn^{2+} (Evans and Moseley, 1985).

Here we give evidence that Mn^{2+} is the optimal cofactor for the UVDE enzymes from *S. pombe*, *B. subtilis* and *T. thermophilus*. Other metals such as Co^{2+} and Ca^{2+} could substitute Mn^{2+}, but to a lesser extend and depending on the type of protein and DNA lesion. Furthermore, we present evidence that the UVDE active site gets fully occupied only after DNA binding. We also compared the activity of the three different UVDE enzymes not only on UV lesions but also on DNA substrates containing an abasic site, a single nucleotide nick or a thymine glycol, showing that the previously reported broad substrate specificity is restricted to the eukaryotic *S. pombe* enzyme.

MATERIALS AND METHODS

Proteins

Plasmid pETUVDEΔ228, encoding residues 229 - 599 of *S. pombe* UVDE, fused to an N-terminal 10 × His tag has been described before (Paspaleva *et al*., 2009). All *S. pombe* UVDE point mutations were constructed by PCR and verified by sequencing for the absence of additional PCR-induced mutations. The mutant UVDE proteins were purified using the same procedure as described for the wild type enzyme (Paspaleva *et al*., 2009) and they all showed the same elution/purification profile.

The *T. thermophilus* UVDE protein was purified as described before (Paspaleva *et al*., 2007).

The *B. subtilis* UVDE gene was amplified by PCR, using primers fusing the C-terminal part of the protein to a 10 × His tag. Subsequently, the gene was inserted into the *Nde*I and *Bam*HI restriction sites of pET11a. The resulting *B. subtilis* UVDE expression vector (pUD17) was transformed into *E.coli* BL21/codon+ (Studier *et al*., 1990). The UVDE protein was purified from cells of a 2 l culture, harvested 2 h after induction by IPTG and lysed by sonication in 6 ml lysis buffer (50 mM Tris pH 7.5, 150 mM NaCl, 10 mM ß-mercaptoethanol, 10 % glycerol, 1 % Triton X-100, 1 % sarcosyl). The lysate was loaded on a HiTrap-chelating Ni column, which was equilibrated with 20 mM Tris pH 7.5. The protein was eluted with a 20 mM to 250 mM imidazole gradient in 20 mM Tris pH 7.5. The UVDE containing fractions were loaded on a hydroxyapatite column, equilibrated with 10 mM KPO_4 (pH 6.5). The protein was eluted with a gradient of 200 mM to 400 mM KPO_4 (pH 6.5). The pooled fractions were subsequently loaded on a P11 phosphocellulose column, equilibrated with 300 mM KPO_4 (pH 6.5) and eluted with 0 M to 1 M gradient of NaCl in the same buffer. Finally, the purified UVDE protein fractions were applied to a Nap™5 gel filtration column (GE Healthcare) and eluted in 20 mM Tris pH 7.5, 150 mM NaCl and 10 % glycerol.

UV survival test

The *Xba*I - *Bam*HI fragments from pETUVDEΔ228 (*S. pombe* UVDE) and pUD17 (*B. subtilis* UVDE) were inserted in pIC-19R, resulting in the expression of the wild type and mutant UVDE proteins under the control of the Plac promoter. The resulting pIC-19R derivatives were introduced in CS 5018 (Δ*uvrA*, Δ*uvrB*) (Moolenaar *et al*., 1994). Cells were grown in LB including 40 µg/ml ampicillin and 1 mM IPTG until OD_{600} of 0.3. The cultures were then diluted ten times and 1 µl drops were spotted on LB plates containing 40 µg/ml ampicillin and 1 mM IPTG. The drops were subsequently irradiated with the indicated dose of UV light and the plates were incubated overnight at 30°C.

DNA substrates

The 30 bp DNA fragments (5'-CTCGTCAGCATC**TT**CATCATACAGTC AGTG-3') with **TT** representing the position of the UV lesion (CPD or 6-4PP) were synthesised as described (Iwai, 2006). The same DNA sequence 5'-CTCGTCAGCATC**X**TCATCATACAGTCAGTG-3', with **X** representing the position of the damage was used for the abasic site (via incorporation of a tetrahydrofuran-dSpacer) or the thymine glycol and obtained commercially (Eurogentec, Belgium). For the studies performed with the ssDNA nick a 50 bp fragment was used 5'-CGTG TGAGGTCGTTCTGAGGTTT*TTTTGTAATGTGCCCGTAAGTAATCCC-3', where the star represents the position of the nick. All substrates containing 2-aminopurine (2 - AP) have been described (Paspaleva *et al*., 2009).

The DNA fragments were 5' radioactively labelled using polynucleotide kinase as described (Verhoeven *et al*., 2002).

Incision assay

The 5' terminally labelled DNA substrates (0.2 nM) were incubated with the indicated amounts of UVDE in a 20 µl reaction mix (20 mM HEPES pH 6.5, 100 mM NaCl) in the presence of the shown amount of divalent metal ions. For some experiments (as specified) the 20 mM HEPES pH 6.5 was substituted with 20 mM Tris with the same pH. After 15 minutes incubation at 30°C (*S. pombe* and *B. subtilis* UVDE) or 55°C (*T. thermophilus* UVDE), the reaction was terminated by adding 3 µl of 0.33 M EDTA, 3.3 % SDS and 2.4 µl glycogen (4 µg / µl), followed by an ethanol precipitation. The incision products were visualised on a 15 % acrylamide gel.

Filter Binding Assay

The filter binding assays were performed in 20 µl samples containing 5 nM or 50 nM UVDE and 4 nM of the terminally labelled DNA substrates in a reaction buffer containing 20 mM Tris pH 6.5, 100 mM NaCl. The mixes were incubated for 10 min at 30°C (*B. subtilis* and *S. pombe* UVDE) or 55°C (*T. thermophilus* UVDE). If needed, metal cofactors (1 mM $MnCl_2$ and/or 10 mM $MgCl_2$) were included in the reaction mix. At the end of the incubation time 0.5 ml of preheated (30°C or 55°C) reaction buffer was added to each sample. The mixture was

subsequently poured over a nitrocellulose filter (Millipore 0.45 µm HA) and the filter was rinsed three times with 0.5 ml of the reaction buffer. Each sample was corrected for the amount of DNA retained on a filter in the absence of protein. Binding is expressed as the percentage of input DNA retained on the filter by the enzymes. For determination of the UVDE binding activity under the conditions used in the 2-AP measurements 4 nM of the terminally labelled substrates were mixed with 0.5 µM unlabeled DNA of the same construct and incubated with *S. pombe* UVDE (2.5 µM) and *B. subtilis* UVDE (2.5 µM or 4 µM) for 10 minutes at 30°C.

2-AP measurements

The 2-AP measurements were conducted in 60-µl samples as described before (Paspaleva *et al*., 2009), using 0.5 µM DNA, 2.5 µM *S. pombe* UVDE and 2.5 µM or 4 µM *B. subtilis* UVDE. The samples were transferred to a 3 mm x 3 mm quartz cuvette and placed in the fluorimeter. Fluorescence emission spectra were obtained using a PerkinElmer LS 50B fluorimeter, connected to a temperature variable water bath to maintain a temperature inside the cuvette of 30°C. The excitation wavelength was set at 310 nm, and the emission spectra were obtained by scanning from 325 to 475-nm.

RESULTS

Mn^{2+} is the optimal UVDE catalytic cofactor for all three enzymes

The similarities between the structures of UVDE from *Thermus thermophilus* (Tth-UVDE) and Endo IV suggest a comparable catalytic mechanism and likely utilization of three metal ion cluster for the DNA cleavage. Although Mn^{2+} was previously shown to be able to bind within the active site of Tth-UVDE and promote catalysis (Paspaleva *et al*., 2007; Meulenbroek *et al*., 2009) it still remains unclear if it is the optimal UVDE cofactor. Furthermore, it is still an open question whether the UVDE proteins from different organisms share the same divalent metal requirements, although as seen in Figure 1 the metal coordinating residues are highly conserved. To obtain a detailed overview of the enzyme cofactor requirements we tested the incision efficiencies of UVDE proteins from *Schizosaccharomyces pombe* (Spo-UVDE), *Bacillus subtilis* (Bsu-UVDE) and *T. thermophilus* (Tth-UVDE) on DNA fragments containing a CPD, a 6-4PP or an abasic site in the presence of different divalent ions (Table 1). The abasic site was chosen to be flanked by two pyrimidines, since it has been shown that the incision activity of Spo-UVDE on this lesion strongly depends on the presence of a neighbouring pyrimidine residue (Paspaleva *et al*., 2009).

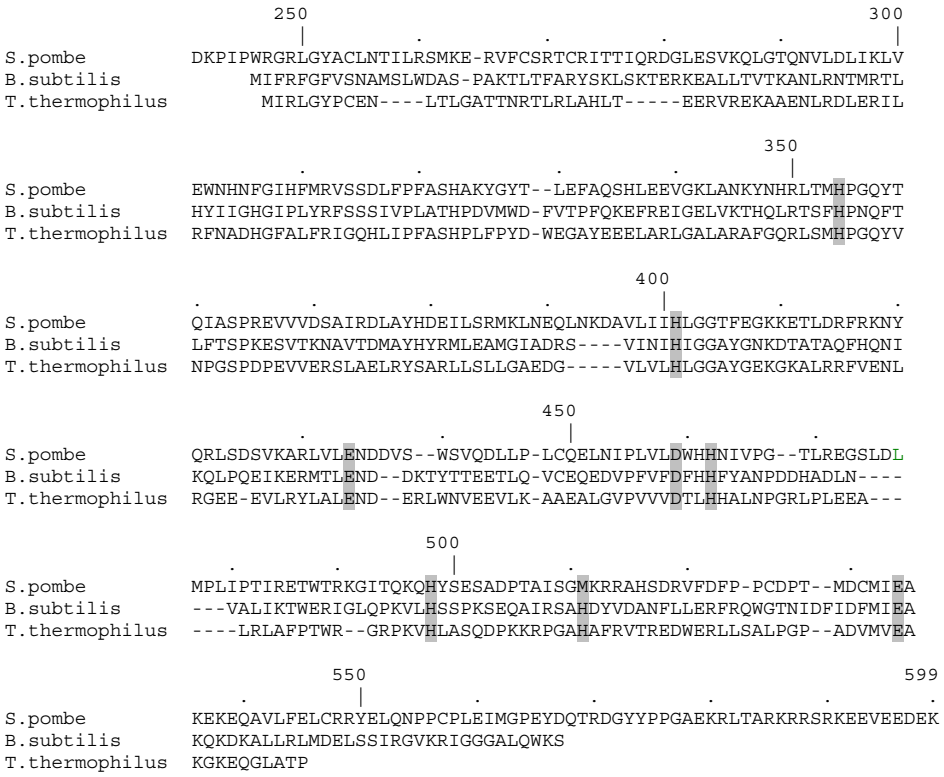

Figure 1: Alignment of the UVDE homologues.

The amino acid sequence of UVDE from *S. pombe* (Takao *et al*., 1996) is aligned with UVDE from *T. thermophilus* (Henne *et al*., 2004) and *B. subtilis* (Kunst *et al*., 1997). The metal coordinating residues are highlighted in grey. The numbering corresponds to the amino acids position in the *S. pombe* UVDE.

As seen in Table 1 (A and B), when Mn^{2+} is added to the reaction mixtures, Spo-UVDE and Bsu- UVDE exhibit similar high activities on all tested DNA damages. In the absence of Mn^{2+} both nucleases do not show any catalytic activity, pointing to the fact that their active sites are not fully occupied with three metal ions. Under this condition the complex formation of both enzymes is comparable, being equally high on the CPD, the 6-4PP and the abasic site (Table 2, A and B). Notably, the amount of protein-DNA complexes is not influenced by the presence of Mn^{2+}, since the binding efficiencies of both proteins are similar in the absence of additional metals or in the presence of Mn^{2+} (Table 2, A and B). This fact highly suggests that full occupation of the UVDE active site is not a requirement for stable DNA binding.

Tth-UVDE shows high incision on substrates containing CPD or 6-4PP, but as previously illustrated (Paspaleva *et al*., 2007), cuts the abasic site containing DNA only 20 % (Table 1C). Interestingly, in the absence of metal ions or in the presence of Mn^{2+} Tth-UVDE distinguishes itself

Table 1: Activity of UVDE enzymes in the presence of different divalent metal ions.

A

Organism: *S. pombe*	-	Mn^{2+}	Co^{2+}	Mg^{2+}	Ca^{2+}	Zn^{2+}	Cu^{2+}
CPD	< 1	97 ± 2	94 ± 2	< 1	5 ± 1	5 ± 2	2
6-4PP	< 1	93 ± 4	79 ± 1	1	20 ± 2	5 ± 1	1
Ap site	< 1	98 ± 1	10 ± 1	< 1	< 1	< 1	< 1

B

Organism: *B. subtilis*	-	Mn^{2+}	Co^{2+}	Mg^{2+}	Ca^{2+}	Zn^{2+}	Cu^{2+}
CPD	< 1	99 ± 1	20 ± 2	< 1	< 1	5 ± 2	10 ± 3
6-4PP	< 1	94 ± 2	50 ± 3	< 1	< 1	< 1	< 1
Ap site	< 1	97 ± 1	2	< 1	< 1	< 1	< 1

C

Organism: *T. thermophilus*	-	Mn^{2+}	Co^{2+}	Mg^{2+}	Ca^{2+}	Zn^{2+}	Cu^{2+}
CPD	< 1	94 ± 1	88 ± 4	< 1	< 1	< 1	< 1
6-4PP	< 1	91 ± 1	50 ± 2	< 1	< 1	< 1	< 1
Ap site	< 1	20 ± 2	20 ± 1	< 1	< 1	< 1	< 1

Incubation was done with 5 nM UVDE and 0.2 nM DNA in the presence of 1 mM of the indicated divalent metal ions or in the absence of additional metals (indicated as -).

as a weak DNA binder, since only 34 % of complex formation is detected on the CPD lesion and about 20 % on the 6-4PP and the abasic site. Even more, at 5 nM protein concentration, which was sufficient to promote 50 % – 60 % binding for Bsu-UVDE and Spo-UVDE, no binding of the Tth-UVDE can be detected at all. Although weak, the Tth-UVDE complex formation is still damage specific, since the complex formation on the undamaged DNA is significantly lower (Table 2C). A probable explanation might be the temperature optimum of the thermophilic enzyme, since it is plausible that at higher temperatures the protein-DNA contacts are weaker and easily disrupted during the experimental procedure. Catalytically the Tth-UVDE is as active as the Bsu- and the Spo-UVDE proteins (Figure 3C), suggesting that transient binding is sufficient for a high incision level. Although the incision of the abasic site by Tth-UVDE is very low, the binding to this substrate is comparable to that observed on the 6-4PP (Table 2C). Apparently both types of damages are equally recognised by the Tth-UVDE enzyme, but subsequent incision cannot efficiently take place at the abasic site.

As seen in Table 1, the highest incision for all tested UVDE proteins is observed in the presence of Mn^{2+}, indicating that it is the optimal UVDE cofactor. Co^{2+} can partially substitute Mn^{2+}, but depending on the lesion and with varying efficiencies for the different UVDE enzymes. For Spo-UVDE Co^{2+} can fully promote activity for the CPD incision, although studies performed with lower protein concentration suggest that Mn^{2+} is slightly more beneficial (data not shown). On the 6-4PP Co^{2+} appears a somewhat less efficient cofactor and on the abasic

Table 2: Binding activity of UVDE enzymes in the presence or absence of additional divalent metals.

A. Spo UVDE

Cofactors:	CPD		6-4PP		Abasic site		Undam.DNA	
	50 nM	5 nM	50 nM	5 nM	50 nM	5 nM	50 nM	5 nM
-	91 ± 1	55 ± 3	92 ± 1	57 ± 1	90 ± 1	53 ± 3	9 ± 1	3 ± 1
Mn^{2+}	94 ± 2	53 ± 2	93 ± 1	60 ± 1	93 ± 2	58 ± 1	23 ± 1	6 ± 1
Mg^{2+}	90 ± 2	50 ± 4	91 ± 2	57 ± 1	85 ± 4	57 ± 2	3 ± 1	1 ± 2
$Mn^{2+} + Mg^{2+}$	94 ± 1	62 ± 2	95 ± 1	66 ± 1	94 ± 1	65 ± 1	11 ± 1	2 ± 2

B. Bsu UVDE

Cofactors:	CPD		6-4PP		Abasic site		Undam.DNA	
	50 nM	5 nM	50 nM	5 nM	50 nM	5 nM	50 nM	5 nM
-	81 ± 2	55 ± 2	86 ± 1	56 ± 3	82 ± 2	60 ± 1	19 ± 2	3 ± 2
Mn^{2+}	80 ± 3	56 ± 2	82 ± 1	59 ± 1	84 ± 2	59 ± 1	40 ± 2	6 ± 2
Mg^{2+}	77 ± 1	51 ± 2	84 ± 1	58 ± 3	79 ± 1	58 ± 3	7 ± 1	3 ± 1
$Mn^{2+} + Mg^{2+}$	82 ± 1	61 ± 3	87 ± 1	67 ± 1	86 ± 1	66 ± 1	21 ± 3	5 ± 2

C. Tth UVDE

Cofactors:	CPD		6-4PP		Abasic site		Undam.DNA	
	50 nM	5 nM	50 nM	5 nM	50 nM	5 nM	50 nM	5 nM
-	34 ± 2	2 ± 1	19 ± 3	< 1	20 ± 2	1 ± 1	3 ± 1	1 ± 1
Mn^{2+}	33 ± 2	1 ± 1	20 ± 1	< 1	23 ± 1	< 1	3 ± 1	1 ± 1
Mg^{2+}	3 ± 1	< 1	4 ± 1	< 1	4 ± 1	< 1	2 ± 1	< 1
$Mn^{2+} + Mg^{2+}$	4 ± 1	< 1	21 ± 1	< 1	20 ± 1	< 1	3 ± 1	< 1

Incubation was done with 4 nM DNA and 50 nM or 5 nM UVDE in the absence of divalent metal ions or in the presence of 1 mM Mn^{2+} and/or 10 mM Mg^{2+} as indicated. The binding is expressed as the percentage of total input DNA.

site its activity is severely reduced (Table 1A). This observation suggests that the type of lesion strongly influences the productive coordination of the divalent metal ions.

Notably, for the Bsu-UVDE Co^{2+} is less capable of replacing Mn^{2+} for its catalytic function on all three substrates. It gives rise to only 20 % incision on the CPD, 50 % on the 6-4PP and hardly any nicking (2 %) on the abasic site (Table 1B). The reduction in the incision efficiency is not due to loss of protein-DNA complexes, since the binding of Bsu-UVDE to damaged DNA is similar in the presence of Co^{2+} or Mn^{2+} (data not shown).

An interesting observation is that for Bsu-UVDE Co^{2+} promotes higher activity on the 6-4PP in comparison with the CPD, while for the Spo enzyme the opposite is observed. Interestingly, Co^{2+} and Mn^{2+} serve as equally good cofactors for the Tth-UVDE incision on the abasic site. Apparently, although the metal coordinating residues are fully conserved, the active sites of Spo-UVDE, Tth-UVDE and Bsu-UVDE might be structurally different.

We also tested a number of other divalent metals for their ability to support the UVDE incisions. As seen in Table 1 Mg^{2+} is not able to promote any detectable incision for all three UVDE enzymes. Both Bsu-UVDE and Spo-UVDE can utilize Zn^{2+} and Cu^{2+}, albeit with very

low efficiency. The Spo protein is the only one from the tested UVDEs, which is able to use Ca^{2+} as a cofactor, but only on the 6-4PP (20 % incision). Bearing in mind the large ionic radius (100 pm) of Ca^{2+} (all other tested divalent metals have ionic radii in the 70 pm range) this shows that Spo-UVDE possesses a remarkable flexibility in its active site. Unlike the other homologues Tth-UVDE is functional only in the presence of Mn^{2+} and Co^{2+}. The reduction of the incision levels is not due to disturbance in the protein-DNA complexes, since the binding of all tested UVDEs in the presence of Mn^{2+}, Co^{2+} or Ca^{2+} is comparable (data not shown).

Taken together, our data clearly demonstrate that for all UVDE proteins the presence of Mn^{2+} is the most beneficial condition in terms of incision efficiency. Other divalent metals, such as Co^{2+} and Ca^{2+} can partially substitute Mn^{2+}, the level of substitution being highly dependent on the DNA lesion and the type of enzyme suggesting structural differences in the active sites of the different UVDE proteins.

Mg^{2+} prevents unspecific binding of Spo- and Bsu-UVDE

Although for many other nucleases it has been shown that Mn^{2+} and Mg^{2+} can substitute each other in function, this is not the case for UVDE. Since no detectable incision for all tested UVDE enzymes was observed with 1 mM Mg^{2+} (Table 1) we also used higher (10 mM) Mg^{2+} concentrations. Under these conditions very low incision is obtained with Spo-UVDE, but only on the UV lesions (Figure 2). Bsu-UVDE doesn't show any nicking and the Tth-UVDE exhibits an extremely low activity on the 6-4PP and no activity on the CPD (Figure 2).

In literature most of the biochemical tests with Spo-UVDE have been performed in the presence of both Mn^{2+} and Mg^{2+} ions suggesting optimal activity under these conditions (reviewed in Doetch *et al*., 2006). Indeed, when we used a lower protein concentration (2 nM), incision on all three substrates by the Spo enzyme is higher in the presence of both 1 mM Mn^{2+} and 10 mM Mg^{2+} than with Mn^{2+} alone (Figure 3A). The same is observed for Bsu-UVDE (Figure 3A). One possible explanation for the observed stimulating effect of Mg^{2+} might be that it becomes part of a catalytically more potent mixed Mn^{2+}/Mg^{2+} active site. Alternatively its effect might not be

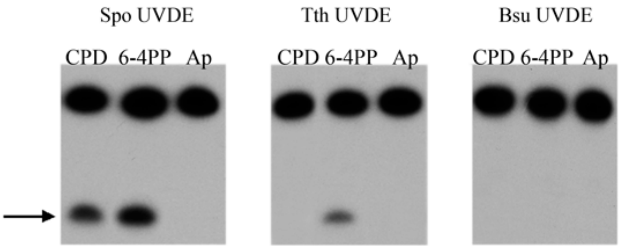

Figure 2: Effect of 10 mM Mg^{2+} on the incision efficiency of different UVDE enzymes.

5 nM of UVDE from *T. thermophilus* (Tth), *S. pombe* (Spo) or *B. subtilis* (Bsu) was incubated for 15 minutes with 0.2 nM DNA substrates containing a CPD, 6-4PP or an abasic site (Ap) lesion in the presence of 10 mM Mg^{2+}. The incision product is indicated with an arrow.

related to a direct binding within the metal coordination site, but to an influence on the stability of the protein-DNA complexes. To discriminate between these two possibilities we performed DNA binding studies in the presence or absence of additional Mg^{2+}.

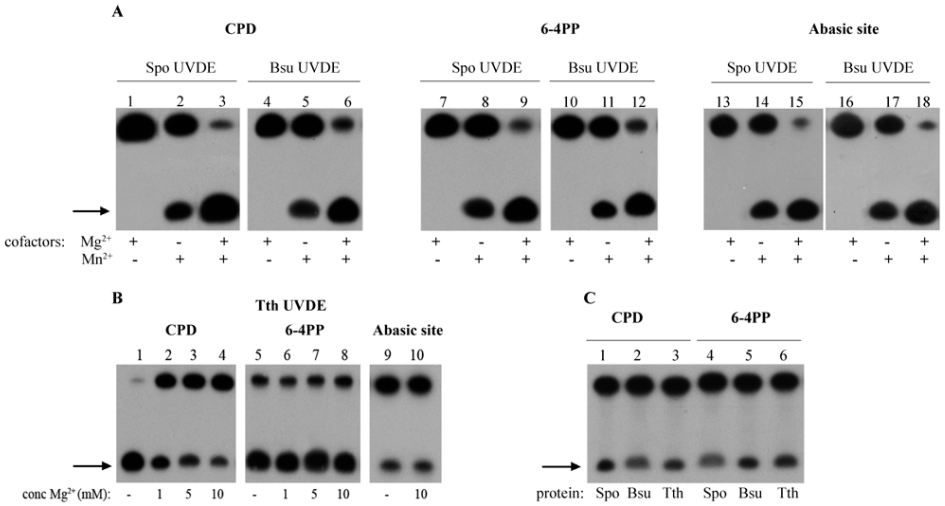

Figure 3: Effect of Mn^{2+} and Mg^{2+} on the incision efficiency of different UVDE enzymes.

A. The UVDE enzymes (2 nM) from *S. pombe* (Spo) and *B. subtilis* (Bsu) were incubated with 0.2 nM DNA containing a CPD, a 6-4PP and abasic site lesions in the presence of 1 mM Mn^{2+} or/and 10 mM Mg^{2+} as indicated.

B. *T. thermophilus* (Tth) UVDE (5 nM) was incubated with the same DNA substrates in the presence of 1 mM Mn^{2+} and different concentration of Mg^{2+} ions as indicated.

C. Spo, Bsu and Tth UVDE (0.25 nM) were incubated for 15 minutes with 0.2 nM CPD and 6-4PP containing DNA fragments. The position of the incision products is shown with arrows.

As shown in Table 2, in the absence of divalent metals the binding of Bsu-UVDE and Spo-UVDE to CPD, 6-4PP and the abasic site is comparably high. Addition of Mg^{2+} or Mn^{2+} alone does not significantly change the amount of detected complexes on any of the tested lesions. With the combination of Mn^{2+} and Mg^{2+}, however, at low protein concentrations (5 nM), a slight stimulating effect is observed.

When we tested the binding of both proteins to undamaged DNA, much more pronounced effect of the metal ions is observed. For both enzymes Mn^{2+} stimulates the unspecific binding at 50 nM of protein (Table 2, A and B). This is an interesting observation, since the role of the metal cofactors is generally limited to the catalytic step and little is known about their influence on the DNA binding. Notably, Bsu-UVDE shows higher affinity for the undamaged DNA substrate than the Spo protein. On the damaged DNA substrates this Mn^{2+} effect is less visible, since it is probably masked by the much stronger impact of the DNA lesion on the enzyme-DNA

interactions. Addition of Mg^{2+} ions at high (50 nM) protein concentrations appears to have an opposite effect on binding to undamaged DNA. As seen in Table 2 (A and B), the binding of Spo-UVDE and Bsu-UVDE to the undamaged DNA in the presence of Mg^{2+} is reduced from 9 % (Spo-UVDE) and 19 % (Bsu-UVDE) to 3 % and 7 % respectively. When both Mn^{2+} and Mg^{2+} ions are present, the binding of Spo- and Bsu-UVDE to undamaged DNA is reduced compared to the incubation with Mn^{2+} alone (Table 2). Taken together, these data indicate that for both Spo-UVDE and Bsu-UVDE Mg^{2+} prevents their unspecific binding, which might explain the stimulating activity of this cofactor on the activities of these enzymes.

To further investigate the effect of Mg^{2+} ions on non-specific UVDE binding we performed competition assays. In these assays undamaged competitor DNA (pUC18) was added in increasing amounts to radioactively labeled DNA fragments containing a CPD (Figure 4, A and C) or 6-4PP (Figure 4, B and D). For both Spo-UVDE and Bsu-UVDE in the absence of divalent metal ions the undamaged competitor slightly reduces the amount of damage-specific complexes formed with CPD and the 6-4PP. When 10 mM Mg^{2+} was included in the reaction the influence of the undamaged DNA is decreased on all tested substrates and the amount of protein-damaged DNA complexes is higher than without metal ions. In the presence of 1 mM Mn^{2+} the amount of specific complexes drastically decreases indicating a Mn^{2+} stimulated binding to the competitor DNA. When both Mn^{2+} and Mg^{2+} ions were included in the reaction mixes the complex formation of Spo-UVDE and Bsu-UVDE on the CPD and the 6-4PP is restored to the level of damage specific binding in the absence of metal ions. This experiment clearly shows that Mn^{2+} severely reduces the ability of the UVDE proteins to discriminate between damaged and undamaged DNA and that the addition of Mg^{2+} ions restores the discriminating properties.

We also tested the UVDE-mediated incision in the presence of non-damaged competitor DNA (Figure 4E). Also in this incision assay the beneficial effect of the ions is clearly visible, since the catalytic activities of both nucleases on the CPD and the 6-4PP are considerably higher with 1 mM Mn^{2+} and 10 mM Mg^{2+} than with Mn^{2+} alone. Under these conditions Mg^{2+} alone cannot support any nicking activity showing once again that it is not a catalytic cofactor for Bsu-UVDE and Spo-UVDE.

Summarizing we can conclude that the beneficial influence of Mg^{2+} on the Spo-UVDE and Bsu-UVDE activities is due to destabilizing the proteins complexes on undamaged DNA sites and not by being part of a mixed Mn^{2+}/Mg^{2+} catalytic site.

Mg^{2+} inhibits the Tth-UVDE active site

When we tested the incision activity of Tth-UVDE in the presence of Mn^{2+} and Mg^{2+}, we did not observe a stimulating effect of Mg^{2+}. Surprisingly on the CPD lesion even an opposite effect was found, since incision was severely reduced in the presence of Mn^{2+} and Mg^{2+} compared to Mn^{2+} alone (Figure 3B, lanes 1 - 4). The inhibitory effect of Mg^{2+} is restricted to the CPD lesion, since as shown in Figure 3B, the nicking activity of this enzyme on the 6-4PP (lanes 5 - 8) and the abasic site (lanes 9, 10) is not influenced by Mg^{2+}.

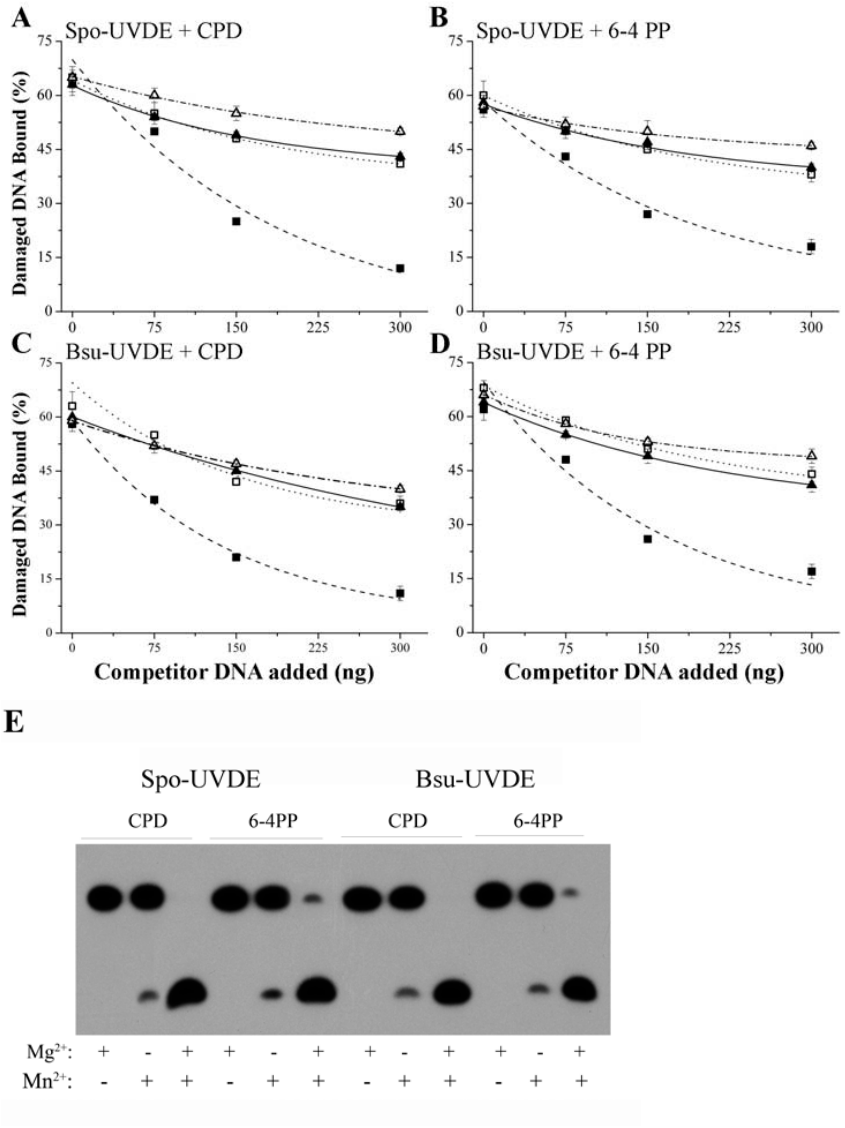

Figure 4: Damage specific binding of Spo-UVDE and Bsu-UVDE in the presence of undamaged competitor DNA.

Radioactively labeled DNA (0.5 nM) containing a CPD (A, C) or a 6-4PP (B, D) was incubated with increasing amounts undamaged cold competitor DNA (pUC18) and 2.5 nM Spo-UVDE (A, B) or Bsu-UVDE (C, D). The DNA was incubated for 10 minutes at 30°C in the absence divalent metals (▲), in the presence of 10 mM Mg^{2+}(△), in the presence of 1 mM Mn^{2+} (■) and in the presence of both 1 mM Mn^{2+} and 10 mM Mg^{2+} (□).

E. DNA fragments (0.5 nM) containing CPD or 6-4PP were incubated with 300 ng undamaged competitor DNA (pUC18) and 2.5 nM Spo-UVDE or Bsu-UVDE in the presence of 1 mM Mn^{2+} and/or 10 mM Mg^{2+}, as indicated. The reactions were stopped after 10 minutes at 30°C and the incision products analysed on a 15 % acrylamide gel.

To discriminate if the influence of Mg^{2+} on Tth-UVDE is pure catalytical or due to a reduced protein-DNA binding, we performed filter binding tests. As discussed before (Table 2C), in the absence of additional metal ions Tth-UVDE appears to be a weak binder compared to the Spo and Bsu enzymes. Addition of 10 mM Mg^{2+} severely decreases the Tth-UVDE complex formation on the CPD from 34 % to 3 %. Mn^{2+} can not rescue the disturbed DNA binding, since only 4 % complexes are observed when both Mn^{2+} and Mg^{2+} are added to the system. Possibly, Mg^{2+} binds within the catalytic site thereby competing with Mn^{2+}. Since the metal cofactors likely participate in the orientation of the DNA substrate within the protein active site this might result in disturbed DNA binding. Strikingly Mg^{2+} can compete with Mn^{2+} even at equimolar concentrations (Figure 3B, lane 2).

The Tth-UVDE binding to the 6-4PP and the abasic site is also reduced with Mg^{2+} alone (Table 2C). In contrast to the CPD lesion, however, Mn^{2+} rescues the 6-4PP and the abasic site binding, since when both Mn^{2+} and Mg^{2+} ions are present, the binding efficiencies are comparable to those with Mn^{2+} alone or in the absence of cofactors (Table 2C).

These data imply that there is a significant difference in the stability of metal ions coordination when Tth-UVDE interacts with CPD on one hand or with 6-4PP and the abasic site on the other. It is very likely that when UVDE is bound to the 6-4PP and the abasic site a stable Mn^{2+} coordination prevents Mg^{2+} from binding in the enzyme metal coordinating sites. In the UVDE-CPD complex, however, Mg^{2+} is capable of removing stable coordination, not only reducing the catalytic efficiency but also the stability of the protein-DNA complexes.

The three UVDE proteins differ in their substrate specificities

We have previously shown that in *E. coli* the repair of UV lesions by the Spo-UVDE protein is very efficient and equals the repair by the UvrABC Nucleotide Excision Repair proteins (Paspaleva *et al*., 2009). To check if that is also the case for the bacterial UVDE homologues we compared the UV survival of NER defective *E. coli* strains expressing Spo-UVDE and Bsu-UVDE. Unfortunately, the Tth homologue could not be tested for *in vivo* activity in *E. coli*, since *in vitro* data showed that this protein is not active at 37°C (data not shown). As seen in Figure 5A, the Spo-UVDE gives rise to a high level of UV resistance, while the Bsu enzyme only partially complements the UV sensitivity of the NER deficient strain. The observed effect is surprising, since both proteins are expressed to the same level (not shown) and they exhibited comparable activity on the 6-4PP and the CPD lesions *in vitro* (Figure 3C). One possibility is that the *in vitro* incubation conditions (pH 6.5) differ from the *in vivo* situation and therefore we tested the activity of both UVDEs at a more physiological pH (7.5). These tests, however, also did not reveal a clear difference between the two enzymes (data not shown). Another explanation for the observed *in vivo* differences might be that the substrate specificity of Spo-UVDE might be broader than that of Bsu-UVDE, including minor UV lesions (other than CPD and 6-4PP). To compare the substrate specificities of Spo-UVDE and Bsu-UVDE we analysed the activities of these enzymes on two other types of DNA modifications, a thymine glycol and DNA containing a single strand nick. These substrates have previously been reported to be incised by the

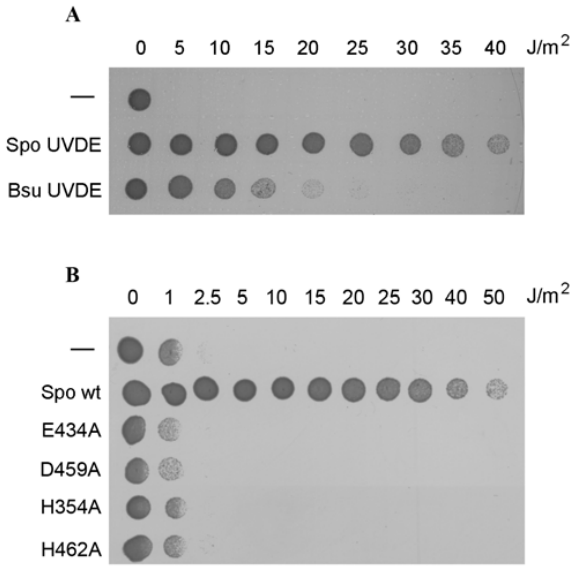

Figure 5: UV survival of *E. coli* strains expressing Spo-UVDE or Bsu-UVDE proteins.

NER deficient (Δ*uvrA*, Δ*uvrB*) *E. coli* cells containing a plasmid expressing the indicated wild type (A) or mutant (B) UVDE proteins were irradiated with different doses of UV light. The empty pUC plasmid was used as a negative control (upper rows).

Spo-UVDE (Paspaleva *et al*., 2009). As seen in Figure 6A, Spo-UVDE shows a moderate activity on the thymine glycol containing fragment (lane 4), but Bsu-UVDE completely fails to incise the DNA containing this damage (lane 3). Furthermore, the Bsu protein also doesn't cut the DNA containing ss-nick (Figure 6B, lane 3), which is a good substrate for the Spo-UVDE (Figure 6B, lane 2).

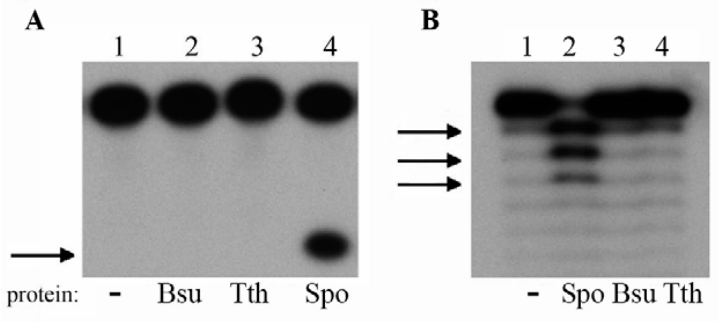

Figure 6: UVDE-mediated incision of DNA substrates containing a thymine glycol or a single strand nick.

A. Tth-, Spo- and Bsu-UVDE enzymes (50 nM) were incubated for 15 minutes with 0.2 nM DNA fragment containing a thymine glycol.

B. DNA containing a ss nick was incubated with 10 nM of the same UVDE proteins. The arrows indicate the position of the incision products.

Despite the lack of incision activity, the binding of the Bsu homologue to the thymine glycol is not significantly different from the complex formation on the CPD and the 6-4PP (Table 3). The complex formation of Bsu-UVDE on single stand nick is reduced, but still significantly higher than on the undamaged DNA. Taken together these finding suggest that Bsu-UVDE is still able to recognize the thymine glycol and the DNA nick as damages, but fails to properly position them in its active site. The same could be true for other types of lesions like other UV induced DNA damages, which might explain the reduced *in vivo* activity of Bsu-UVDE.

Table 3: Binding efficiencies of UVDE enzymes on different DNA lesions.

DNA damage:	Spo	Bsu	Tth
No	3 ± 1	3 ± 2	3 ± 1
CPD	55 ± 3	55 ± 2	34 ± 2
6-4PP	57 ± 1	56 ± 3	19 ± 1
Abasic site	53 ± 3	60 ± 1	20 ± 2
Thymine glycol	58 ± 1	50 ± 2	4 ± 1
DNA nick	52 ± 1	39 ± 2	3 ± 3

DNA with the indicated damage was incubated with 50 nM Tth-UVDE, 5 nM Spo-UVDE or 5 nM Bsu-UVDE for 10 minutes in the absence of divalent metal ions.

We also tested the Tth-UVDE on the thymine glycol and DNA containing a single strand nick. As seen in Figure 6 A, B (lane 4), it not only completely failed to incise the two substrates but it can no longer discriminate this damage from undamaged DNA (Table 3). Since the Tth protein outlines itself as a weak binder even on substrates introducing major changes in the DNA structure such as the 6-4PP, the structural changes induced by a nick or a thymine glycol most likely are not sufficient to promote proper DNA binding.

In conclusion, Spo-UVDE distinguishes itself from its bacterial homologues with a much broader substrate specificity. Bsu-UVDE is more restricted, although in addition to the CPD and 6-4PP, it can also incise an abasic site. The Tth enzyme, however, can only efficiently repair CPD and 6-4PP lesions.

Dynamics of Spo and Bsu UVDE pre-incision complexes

Previously we have shown by using 2-aminopurine (2-AP) fluorescence studies that the Spo-UVDE causes significant destacking of the two bases opposite a CPD and a 6-4PP (Paspaleva *et al*., 2009). Similar conformational changes were observed with the base facing the abasic site. Furthermore, quenching experiments with acrylamide revealed that these bases in the non-damaged strand do not become solvent exposed and are in a contact with side chains of the protein.

To see if similar conformational changes occur upon Bsu-UVDE binding to these damages we compared the 2-AP fluorescence in the presence of this enzyme to that induced by Spo-UVDE. For this purpose we used DNA fragments containing 2-AP incorporated at two positions

opposite a CPD, 6-4PP or an abasic site. The presence of the 2-AP did not change the incision efficiencies of either Bsu-UVDE or Spo-UVDE (data not shown). The binding properties of both nucleases are also not altered by the presence of the 2-AP (Table 4).

Table 4: *S. pombe* and *B. subtilis* UVDE binding on 2-AP containing DNA substrates.

Damage	2-AP position	% binding Spo	% binding Bsu
CPD	no	61 ± 1	62 ± 1
CPD	1	60 ± 1	62 ± 1
CPD	2	59 ± 1	57 ± 3
6-4PP	no	59 ± 3	63 ± 1
6-4PP	1	61 ± 4	61 ± 3
6-4PP	2	65 ± 1	64 ± 2
Abasic site	no	62 ± 1	62 ± 2
Abasic site	1	61 ± 4	61 ± 1
Abasic site	2	60 ± 1	62 ± 3
Thymine glycol	no	60 ± 1	58 ± 2
Thymine glycol	1	60 ± 2	57 ± 2
Thymine glycol	2	61 ± 1	58 ± 1
Nick	no	57 ± 1	54 ± 2
Nick	1	57 ± 2	55 ± 3
Nick	2	59 ± 1	58 ± 1

The incubations were done using the same conditions as used for the fluorescence assays without metal cofactors. The binding is expressed as the percentage of total input DNA retained on a filter.

In the absence of protein the CPD, the 6-4PP and the abasic site lesion containing fragments do not exhibit significant fluorescence (Figure 7, A - F), showing that these damages do not disturb the base stacking in the opposing strand. As previously shown (Paspaleva *et al*., 2009), the 2-AP signal in the presence of Spo-UVDE is significantly increased at both positions. In comparison, the Bsu-UVDE also causes notable change in the 2-AP fluorescence, suggesting that like Spo-UVDE this homologue is also able to cause destacking of the bases opposite the DNA damage. There are, however, multiple differences between Spo-UVDE and Bsu-UVDE. The levels of destacking differ depending on the damage. For instance upon incubation of the CPD and the AP site containing DNA with Bsu-UVDE the fluorescence of the 2-AP at position 1 is lower than the one caused by the Spo homologue (Figure 7, A and E), whereas the signal at position 2 is notably higher (Figure 7, B and F). Both proteins, however, cause a more pronounced effect on position 2. On the 6-4PP containing fragment Bsu-UVDE has a higher impact on the 2-AP at position 1, compared to the CPD and the AP site containing fragments, but the signal is still lower compared to Spo-UVDE (Figure 7C). Also the signal at position 2 is now lower than that of Spo-UVDE (Figure 7D). Another striking difference between the Spo and the Bsu enzymes is that for both 2-AP residues the emission maximum in the Bsu-UVDE and Spo-UVDE complexes are shifted with respect to each other by ~ 50 nm.

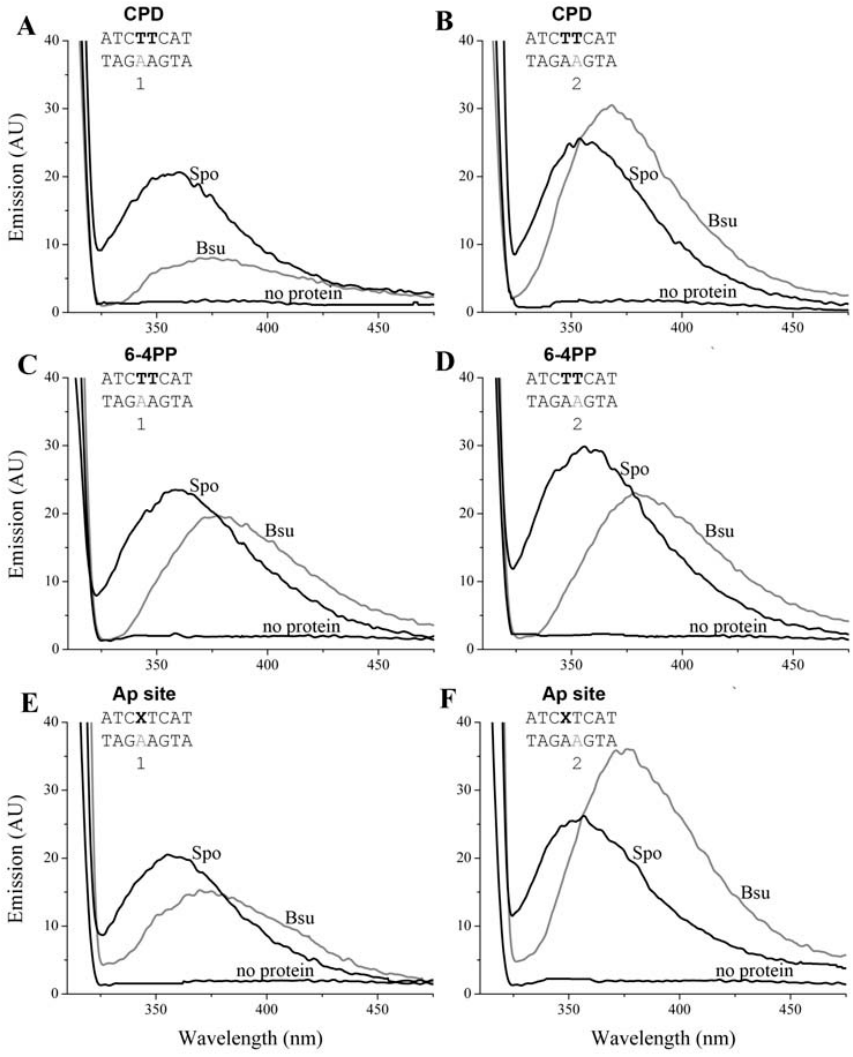

Figure 7: Fluorescence emission spectra of UVDE-DNA complexes.

The DNA fragments (0.5 μM) with a CPD (A and B), 6-4PP (C and D) or an abasic site (E and F) were incubated with or without 2.5 μM Spo-UVDE and Bsu-UVDE for 10 minutes at 30°C. Panels A, C and E show the 2-AP signal when the fluorescent base is positioned directly opposite the 5'T of the CPD and the 6-4PP or opposite the abasic site, while in panels B, D and F the 2-AP is incorporated opposite the 3'T of the CPD, 6-4PP and the 3' neighbor of the abasic site.

When we added the quenching agent acrylamide in our incubation mixes we couldn't detect any change in the 2-AP fluorescence in either of the Spo-UVDE or Bsu-UVDE complexes (data not shown). Apparently in both enzymes the bases in the non-damaged strand are shielded from the solution by protein side chains. The way that this is achieved, however, might be different

for the two proteins as illustrated by the shift in emission maximum, which is indicative of a different polaritiy in the environment op the 2-AP residues (Ward *et al*., 1969).

Next we compared the activity of both enzymes on DNA fragments where the 2-AP was incorporated opposite a thymine glycol and ssDNA nick. As shown before (Paspaleva *et al*., 2009), although the CPD, the 6-4PP and the abasic site do not cause destacking in the undamaged strand by themselves this is not the case for a ss nick or a thymine glycol, where in an absence of protein a fluorescent signal of 15 AU and 10 AU, respectively is observed (Figure 8). The Spo-UVDE causes a significant destabilization in the undamaged DNA strand of a thymine glycol containing DNA (Figure 8, A and B) and again addition of acrylamide did not reduce the fluorescence signal (Paspaleva *et al*., 2009). In contrast the Bsu-UVDE doesn't not cause any detectable destacking in the undamaged strand of the thymine glycol containing fragment (Figure 8, A and B). This is not due to a lack of protein-DNA complexes, since filter binding studies revealed that at the conditions used 58 % of the DNA is bound by the Bsu-UVDE (Table 4).

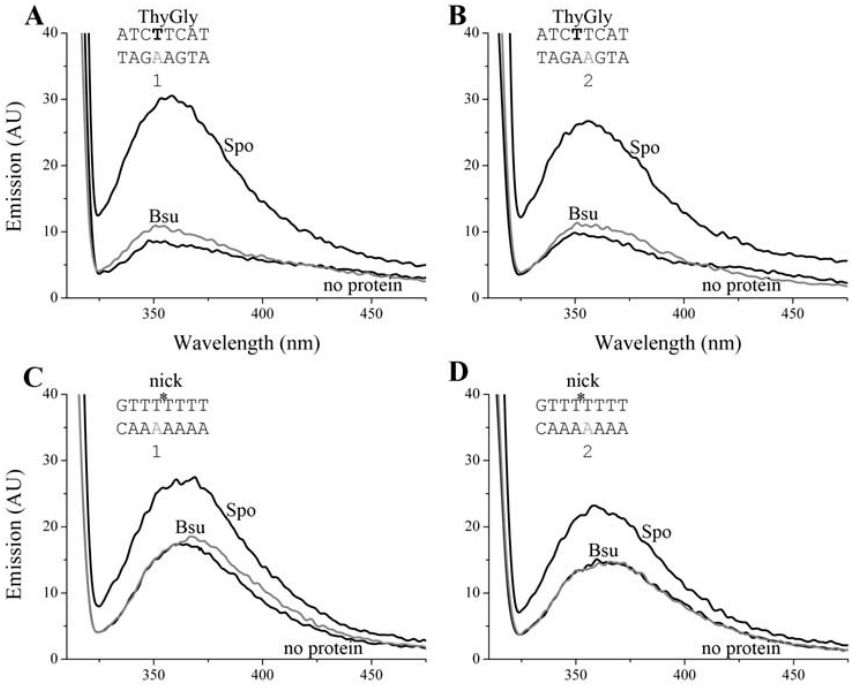

Figure 8: Fluorescence emission spectra of UVDE-DNA complexes.

DNA (0.5 μM) containing a thymine glycol (A and B) or ss nick (C and D) was incubated with 2.5 μM Spo-UVDE and 4 μM Bsu-UVDE for 10 minutes at 30°C. In panels A, C the 2-AP is placed opposite the base flanking the nick on the 5' side or directly opposite the thymine glycol. In panels B, D the fluorescent base faces the nucleotide on the 3' side of the nick or the 3' neighbor of the thymine glycol.

A similar result was obtained with the two 2-AP residues opposite the two T's flanking a nick (Figure 8, C and D). Whereas Spo-UVDE does cause destacking of these bases, Bsu-UVDE fails to induce any change in fluorescence despite the 55 % binding efficiency (Table 4). Apparently Bsu-UVDE does recognize a DNA fragment containing a thymine glycol or a nick, but is not able to induce conformational changes in the opposing strand, which might explain why this protein fails to incise these DNA damages.

We also performed fluorescence studies with the Tth-UVDE, however no change of the 2-AP signal was detected on any of the substrates. The amount of complexes detected under the fluorescence conditions (~ 15 %) is probably too low.

Active site organization of Spo UVDE

Based on sequence alignment of Spo-UVDE, Bsu-UVDE and the known metal coordinating residues in Tth-UVDE, it is likely that in Spo-UVDE Mn1 is coordinated by Glu434, Glu535, His498, Asp459 (Figure 1). Mn2 is oriented with the help of Glu434, His354 and His401 and according to the alignment Mn3 must be in a contact with Met511 and His462. Methionine, however, is very unlikely to act as a metal coordinator and possibly in Spo-UVDE this role is performed by His516. All metal coordinators, except the one replaced by methionine in the Spo-UVDE sequence, are highly conserved (Figure 1). The importance of Mn1 for Spo-UVDE function was previously demonstrated, since alanine substitutions of Glu434 and Asp459 abrogated the catalytic activity of the enzyme (Paspaleva *et al*., 2007). To test the importance of the other metals we made additional substitutions of His354 and His462. As expected the resulting mutant proteins are disturbed in incising DNA containing an abasic site (Table 5) with H462A showing a 50 % reduction and H354A completely failing to incise the abasic site lesion. On the CPD and the 6-4PP, however, the activity of the mutants is comparable to the wild type protein (Table 5). Once again this shows that the metal coordination is influenced by the type of lesion. Apparently in the mutant proteins the three metal ions can still be properly positioned at the UV-lesions but not on the abasic site.

Surprisingly all Spo-UVDE active site mutants, including H354A and H462A appeared completely repair deficient *in vivo* (Figure 5B). One possible explanation for the discrepancy between the *in vivo* and the *in vitro* data might be that the conditions used in our incision assays

Table 5: Effect of the pH on the incision activity of wild type and mutant UVDE enzymes.

	CPD		6-4PP		Abasic site
UVDE	pH 6.5	pH 7.5	pH 6.5	pH 7.5	pH 6.5
wild type	97 ± 2	97 ± 1	95 ± 1	95 ± 2	95 ± 1
H354A	97 ± 3	20 ± 1	95 ± 2	20 ± 3	<1
E434A	< 1	< 1	< 1	< 1	<1
D459A	< 1	< 1	< 1	< 1	<1
H462A	97 ± 1	10 ± 3	95 ± 3	10 ± 1	50 ± 4

Incubation was done with 5 nM UVDE enzymes and 0.2 nM DNA in the presence of 1 mM Mn^{2+} and 10 mM Mg^{2+} at pH 6.5 and pH 7.5. The numbers represent the incision percentages.

differ from the *in vivo* situation. The cellular pH of *E. coli* is around 7.5 (Padan *et al*., 1981). In literature the optimal pH for the Spo-UVDE was reported to be 6.5 (Kaur *et al*., 1998) and all incision and DNA binding assays have therefore been performed in a buffer of this lower pH. To test if indeed the pH might be an explanation for the observed differences we tested the incision efficiency of Spo-UVDE at pH 7.5 and pH 6.5. As shown before (Paspaleva *et al*., 2009) the higher pH does not influence the incision activity of the wild type Spo enzyme on any of the tested lesions (Table 5). However, when we tested the activity of Spo active site mutants at pH 7.5, the incision activities of both H354A and H462A are significantly reduced (Table 5). The damage-specific binding of the mutants, however, is not altered by the pH (Table 6). Apparently the metal coordination in the UVDE active site is strongly influenced by the pH, most likely by influencing the position of the amino acid residues, which participate in the metal ions coordination.

Table 6: Effect of the pH on the DNA binding properties of wild type and mutant Spo-UVDE enzymes.

UVDE	Undam. DNA *		CPD		6-4PP		Abasic site	
	pH 6.5	pH 7.5	pH 6.5	pH 7.5	pH 6.5	pH 7.5	pH 6.5	pH 7.5
wild type	9 ± 1	6 ± 3	55 ± 3	52 ± 2	57 ± 1	57 ± 4	56 ± 1	59 ± 2
H354A	11 ± 2	9 ± 3	52 ± 4	53 ± 1	60 ± 2	57 ± 3	60 ± 2	58 ± 2
E434A	7 ± 3	5 ± 2	53 ± 1	49 ± 1	59 ± 2	56 ± 3	61 ± 1	57 ± 2
D459A	10 ± 2	7 ± 1	58 ± 1	54 ± 4	61 ± 3	58 ± 1	59 ± 1	62 ± 2
H462A	7 ± 1	6 ± 1	54 ± 1	51 ± 3	61 ± 2	61 ± 2	58 ± 2	62 ± 1

*Incubation on the undamaged DNA was done with 50 nM Spo UVDE and 4 nM DNA.

The incubation on the CPD, 6-4PP and the abasic site lesion was performed with 5 nM UVDE and 4 nM DNA fragments. All incubations were done in the absence of additional metals. The binding is expressed as the percentage of total input DNA.

DISCUSSION

The recently solved UVDE structure from *T. thermophilus* (Paspaleva *et al*., 2007) outlined the presence of three divalent metals and crystallisation trials in the presence of 1 mM Mn^{2+} showed that the three metal binding sites have the potential to be all occupied by Mn^{2+}, forming a compact cluster (Meulenbroek *et al*., 2009). However, it was not clarified if Mn^{2+} is indeed the enzyme's optimal catalytic cofactor. In our study we not only give direct evidence that Mn^{2+} is the actual UVDE cofactor, but we also show which other metals can substitute the Mn^{2+} ions. In our tests Co^{2+} is revealed to be one of the most effective substitutes for Mn^{2+}, not only for the Spo protein, but also for Tth-UVDE and to a lesser extend for Bsu-UVDE. Notably Cu^{2+} and Zn^{2+}, which are highly similar in ionic radius and exhibit the same charge as Co^{2+} can support only a very low enzymatic activity, thus the ionic radius, although important, is not the only decisive factor for the metal function.

Spo-UVDE distinguishes itself from Bsu- and Tth-UVDE by being able to use Ca^{2+} as a metal cofactor. The large ionic radius of Ca^{2+} makes it highly unlikely that a cluster of three Ca^{2+} ions is formed in the catalytic site of UVDE. Possibly Ca^{2+} can be part of mixed Mn^{2+}/Ca^{2+} active site, making use of one or more intrinsically bound Mn^{2+} ions. An active complex, however, could only be formed on the 6-4PP indicating that the DNA itself has a major role in the coordination of the metal ions (see also below).

Both Bsu and Tth proteins exhibit more stringent divalent metal requirements compared to the Spo orthologue. From the three nucleases Tth-UVDE has the most restricted metal requirement as incision is supported only in the presence of Mn^{2+} or Co^{2+}. However, bearing in mind that binding of divalent metals is expected to be temperature dependent, the incubations of the thermophyllic protein at 55°C might negatively influence stable coordination of other cofactors.

An intriguing observation is that most of the tested divalent metal ions have been found to support different levels of UVDE activity, depending on the type of damage in the DNA substrate. This indicates that the DNA itself assists in the coordination of the metal ions, implying that at least part of these metal ions bind into the active site after association of the protein with the DNA. The crystal structure of the Tth-UVDE protein revealed the presence of a phosphate ion coordinated by all three Mn^{2+} ions (Paspaleva *et al*., 2007). Most likely this phosphate ion represents a phosphate of the DNA backbone in the protein-DNA complex. Positioning of this DNA-phosphate is likely to be dependent on the type of DNA lesion explaining why metal coordination is dependent on the DNA substrate. This model is supported by the properties of the Spo-UVDE active site mutant H354A (coordinator of Mn2), which is completely deficient in nicking the abasic site but shows wild type level of incision on the CPD and the 6-4PP, again showing that metal coordination is stabilised via the DNA.

In our studies we were also able to distinguish between metal ions needed to occupy the active site and metal ions affecting the DNA binding. Mg^{2+} although used by some authors in UVDE incision assays (Kanno *et al*., 1999), can support incision activity only in the case of the Spo homologue and even then a higher concentration of Mg^{2+} ions (10 mM) is needed. One likely explanation is the reported high charge density of Mg^{2+}, which poses a strong electrostatic barrier for formation of a three ions Mg^{2+} cluster (Cowan, 2002). The fact that Spo-UVDE can still use this metal ion for catalysis suggests that a mixed Mg^{2+}/Mn^{2+} metal binding site is possible for this nuclease. This in combination with the ability of Spo-UVDE to perform incision in the presence of numerous other divalent metals underlines a high flexibility of its active site.

In our DNA binding experiments we showed that Mg^{2+} has a role in preventing the binding of Spo- and Bsu-UVDE to undamaged DNA, thereby enhancing its damage-specific incision. Therefore for both nucleases the combination of Mn^{2+} and Mg^{2+} provides the optimal reaction condition: Mn^{2+} acting as a pure catalytic cofactor and Mg^{2+} as a DNA binding modifier. A reducing effect of Mg^{2+} on non-specific DNA binding has also been described for other enzymes, like the B-ZIP transcription factor (Moll *et al*., 2002) and the restriction nuclease *Eco*RV (Jeltsch *et al.,* 1997). Mg^{2+} has been shown to binds to the phosphates of the DNA backbone (Cowan,

1998; Hackl *et al*., 2005) and needs to be released upon protein binding. The interaction of UVDE at non-specific sites is expected to be mainly via these phosphates, hence interference by the Mg^{2+} ions. Damage specific binding, as expected for a non-sequence specific protein, will also involve phosphate contacts. In addition, however, the complex will be stabilised by other factors like DNA kinking and specific interactions with the damaged bases in the active site (see also below), compensating for the inhibitory effect of Mg^{2+}.

Mn^{2+} appeared to have an opposite effect on DNA binding as it was seen to stimulate binding to undamaged DNA. Although Mn^{2+} also binds to DNA it was shown to have a higher affinity for the DNA bases causing destabilisation and bending of the DNA (Polyanichko *et al*., 2004; Hackl *et al*., 2005). Since, as described before (Paspaleva *et al*., 2009) UVDE binds to sites, which allow DNA bending, Mn^{2+} might promote unspecific binding of the protein by altering the DNA flexibility.

For Tth-UVDE the additional presence of Mg^{2+} resulted in a severe reduction of incision on the CPD, whereas the activity on the 6-4PP was not affected. It is very unlikely that the negative effect of Mg^{2+} is due to an influence on specific protein-DNA contacts (i.e. competing for phosphate binding), since in the absence of cofactors the protein-DNA complex on the CPD is even more stable than on the 6-4PP. More likely Mg^{2+} becomes part of a mixed Mg^{2+}/Mn^{2+} active site leading to a catalytically inactive protein. Since, as discussed above, metal coordination is highly dependent on the type of substrate the disturbing coordination of Mg^{2+} does not take place on the 6-4PP. Strikingly the hampering effect of Mg^{2+} on CPD incision was already apparent at equimolar concentrations of 1 mM, making it questionable whether *in vivo* the Tth-UVDE would be capable of repairing CPD at all. Although the concentration of free Mg^{2+} in the *T.thermophilus* cells is rather low: 1.53 mM (Kondo *et al*., 2007) or according to other authors (Wakamatsu *et al*., 2007) even lower (0.53 mM), it is not very likely that it will be greatly exceeded by the concentration of Mn^{2+} (which until now has not been determined). In that regard it is possible that *in vivo* the UVDE enzyme of *T. thermophilus* will only repair 6-4PP lesions.

The three UVDE homologues show very different *in vitro* substrate specificity. Spo-UVDE is not only active on CPD, 6-4PP and abasic sites, but also on thymine glycol and DNA containing a nick. We have, however, previously shown (Paspaleva *at al*., 2009) that incision of the DNA containing a nick or abasic site is highly dependent on the presence of flanking pyrimidines. It was therefore proposed that in order to position the scissile phosphodiester bond into the active site, the damaged nucleotides have to be rotated into a pocket of the protein, which is located at the bottom of a proposed DNA binding groove (Paspaleva *at al*., 2007). Purine residues will be excluded from this pocket making the protein selective for (distorted) pyrimidines or an abasic site together with a pyrimidine. Most likely the complex will be further stabilised by contacts of the rotated pyrimidine(s) with side chains of the protein pocket. The substrate specificity of the Bsu homologue appears to be more limited. Although the DNA containing a CPD, 6-4PP or abasic site are efficiently incised no activity on DNA with a thymine glycol or single strand nick

could be detected. A clue for what might cause the difference between the two proteins came from studying conformational changes in the opposing strand using the fluorescent residue 2-AP. Previously, it was shown with Spo-UVDE that Tyr358 causes destacking of bases opposing the lesion. A model was proposed in which Tyr358 will wedge between the two residues opposite the damage thereby disturbing the base stack and stabilizing the DNA kink (Paspaleva *at al*., 2009). With Bsu-UVDE a similar destacking of bases opposite the CPD, 6-4PP or abasic site was observed but the protein appeared incapable of inducing a conformational change of bases opposing a nick or thymine glycol. Tyr358 is part of a GQY loop, which in the crystal structure of Tth-UVDE is located at the bottom of a proposed DNA binding groove. Although this loop is conserved in the Spo and Tth proteins the sequence of the corresponding region in Bsu-UVDE is NQF (Figure 1). Although the corresponding phenylalanine in Bsu-UVDE can fulfil a similar wedging function as Tyr358, the positioning of this residue might be different as a result of the presence of an asparagine instead of a glycine in the NQF loop. That indeed on the CPD, 6-4PP and abasic site the Phe residue of Bsu-UVDE is positioned differently was not only evident from a difference in the level of the fluorescence signals induced by the Spo- and Bsu proteins. More strikingly the emission maximum of the 2-AP residues was shifted by about 50 nm indicating that the bases in the non-damaged strand are placed in a different amino acid context. Possibly this different NQF loop could also be the reason that Bsu-UVDE is incapable of causing destacking of the bases opposing a thymine glycol or single-strand nick. As a consequence also the damage itself is not properly positioned into the active site of the protein and subsequent incision cannot take place.

The Tth-UVDE shows the most restricted substrate specificity, only efficiently incising the CPD and 6-4PP. The protein-DNA complexes formed by Tth-UVDE appeared much more instable so we could not test whether also for this protein the substrate specificity is related to the capacity to induce destacking of bases in the non-damaged strand. Because the high temperature used for Tth-UVDE will inflict more flexibility in the DNA, this protein might be more dependent on direct interactions with the damaged nucleotides for proper positioning of the scissile phosphodiester bond. The absence of an interacting base in the abasic site substrate could then explain its lower incision efficiency on this DNA.

REFERENCES

Bowman KK, Sidik K, Smith CA, Taylor JS, Doetsch PW, Freyer GA, A new ATP-independent DNA endonuclease from *Schizosaccharomyces pombe* that recognizes cyclobutane pyrimidine dimers and 6-4 photoproducts, *Nucleic Acids Res*. **22** (1994), pp. 3026-3032

Cowan JA, Structural and catalytic chemistry of magnesium-dependent enzymes, *Biometals* **15** (2002), pp. 225-235

Doetsch PW, Beljanski V and Song B, The ultraviolet damage endonuclease (UVDE) protein and alternative excision repair: a highly diverse system for damage recognition and processing. In: V. Beljanski and B. Song, Editors, *DNA Damage Recognition*, Taylor & Francis Press, New York (2006), pp. 211-223

Evans DM, Moseley BE, Identification and initial characterisation of a pyrimidine dimer UV endonuclease (UV endonuclease beta) from *Deinococcus radiodurans*; a DNA-repair enzyme that requires manganese ions, *Mutat Res*. **145** (1985), pp. 119-128

Goosen N, Moolenaar GF, Repair of UV damage in bacteria, *DNA Repair* **7** (2008), pp. 353-379

Hackl EV, Kornilova SV, Blagoi YP, DNA structural transitions induced by divalent metal ions in aqueous solutions, *Int J Biol Macromol*. **35** (2005), pp. 175-191

Henne A, Bruggemann H, Raasch C, Wiezer A, Hartsch T, Liesegang H, Johann A, Lienard T, Gohl O and Martinez-Arias R, *et al*., The genome sequence of the extreme thermophile *Thermus thermophilus*, *Nat*. *Biotechnol*. **22** (2004), pp. 547-553

Hosfield DJ, Guan Y, Haas BJ, Cunningham RP and Tainer JA, Structure of the DNA repair enzyme Endo IV and its DNA complex: double-nucleotide flipping at abasic sites and three-metal-ion catalysis, *Cell* **98** (1999), pp. 397-408

Iwai S, Chemical synthesis of oligonucleotides containing damaged bases for biological studies, *Nucleosides Nucleotides Nucleic Acids* **25** (2006), pp. 561-582

Jeltsch A, Maschke H, Selent U, Wenz C, Köhler E, Connolly BA, Thorogood H, Pingoud A, DNA binding specificity of the *Eco*RV restriction endonuclease is increased by Mg^{2+} binding to a metal ion binding site distinct from the catalytic center of the enzyme. *Biochemistry* **34** (1995), pp. 6239-6246

Kanno S, Iwai S, Takao M, Yasui A, Repair of apurinic/apyrimidinic sites by UV damage endonuclease; a repair protein for UV and oxidative damage, *Nucleic Acids Res*. **27** (1999), pp. 3096-3103

Kaur B, Fraser JL, Freyer GA, Davey S, Doetsch PW, A Uve1p-mediated mismatch repair pathway in *Schizosaccharomyces pombe*, *Mol Cell Biol*. **19** (1999), pp. 4703-4710

Kondo N, Nishikubo T, Wakamatsu T, Ishikawa H, Nakagawa N, Kuramitsu S, Masui R, Insights into different dependence of dNTP triphosphohydrolase on metal ion species from intracellular ion concentrations in *Thermus thermophilus*, *Extremophiles*. **12** (2008), pp. 217-223

Kunst F, Ogasawara N, Moszer I, Albertini AM, Alloni G, Azevedo V, Bertero MG, Bessieres P, Bolotin A and Borchert S, *et al*., The complete genome sequence of the Gram-positive bacterium *Bacillus subtilis*, *Nature* **390** (1997), pp. 249-256

Kutyavin IV, Milesi D, Belousov Y, Podyminogin M, Vorobiev A, Gorn V, Lukhtanov EA, Vermeulen NM, Mahoney W, A novel endonuclease IV post-PCR genotyping system, *Nucleic Acids Res*. **34** (2006), pp. 28-134

Levin JD, Johnson AW, Demple B, Homogeneous Escherichia coli endonuclease IV. Characterization of an enzyme that recognizes oxidative damage in DNA, *J Biol. Chem*. **263** (1988), pp. 8066-8071

Levin JD, Shapiro R, Demple B, Metalloenzymes in DNA repair. *Escherichia coli* endonuclease IV and *Saccharomyces cerevisiae* Apn1, *J Biol. Chem*. **266** (1991), pp. 22893-22898

Meulenbroek EM, Paspaleva K, Thomassen E, Abrahams JP, Goosen N, Pannu NS, Involvement of a carboxylated lysine in UV damage endonuclease, *Protein Science*, (2009), in press

Moll JR, Acharya A, Gal J, Mir AA, Vinson C, Magnesium is required for specific DNA binding of the CREB B-ZIP domain, *Nucleic Acids Res*. **30** (2002), 1240-1246

Moolenaar GF, Visse R, Ortiz-Buysse M, Goosen N, van de Putte P, Helicase motifs V and VI of the *Escherichia coli* UvrB protein of the UvrABC endonuclease are essential for the formation of the preincision complex, *J Mol Biol*. **240** (1994), pp. 294-307

Padan I, Zilberstein D, Schuldiner S, pH homeostasis in bacteria, *Biochim*. *Biophys*. *Acta* **650** (1981), pp. 151-166

Paspaleva K, Moolenaar GF, Goosen N, Damage recognition by UV damage endonuclease from *Schizosaccharomyces pombe*, *DNA Repair* (2009), in press

Paspaleva K, Thomassen E, Pannu NS, Iwai S, Moolenaar GF, Goosen N, Abrahams JP, Crystal structure of the DNA repair enzyme ultraviolet damage endonuclease, *Structure* **15** (2007), pp. 1316-1324

Polyanichko AM, Andrushchenko VV, Chikhirzhina EV, Vorob'ev VI, Wieser H, The effect of manganese(II) on DNA structure: electronic and vibrational circular dichroism studies, *Nucleic Acids Res*. **32** (2004), pp. 989-996

Studier FW, Rosenberg AH, Dunn JJ, Dubendorff JW, Use of T7 RNA polymerase to direct expression of cloned genes, *Methods Enzymol*. **185** (1990), pp. 60-89

Takao M, Yonemasu R, Yamamoto K and Yasui A, Characterization of a UV endonuclease gene from the fission yeast *Schizosaccharomyces pombe* and its bacterial homolog, *Nucleic Acids Res*. **24** (1996), pp. 1267-1271

Verhoeven EE, van Kesteren M, Turner JJ, van der Marel GA, van Boom JH, Moolenaar GF and Goosen N, The C-terminal region of Escherichia coli UvrC contributes to the flexibility of the UvrABC nucleotide excision repair system, *Nucleic Acids Res*. **30** (2002), pp. 2492-2500

Wakamatsu T, Ishikawa H, Nakagawa N, Kuramitsu S, Masui R, Intracellular ion concentrations in *Thermus thermophilus*, *Extremophiles* **15** (2008), pp. 317-323

Ward DC, Reich E, Streyer L, Fluorescence studies of nucleotides and polynucleotides. I. Formycin, 2-aminopurine riboside, 2,6-diaminopurine riboside and their derivatives, *J Biol Chem*. **244** (1969), pp. 1228-1237